Magnetobiostratigraphic chronology of the Eocene–Oligocene transition in the CIROS-1 core, Victoria Land margin, Antarctica: Implications for Antarctic glacial history

Gary S. Wilson* *Byrd Polar Research Center, Ohio State University, 1090 Carmack Road, Columbus, Ohio 43210*

Andrew P. Roberts *Department of Oceanography, University of Southampton, Southampton Oceanography Centre, European Way, Southampton SO14 3ZH, United Kingdom*

Kenneth L. Verosub *Department of Geology, University of California, Davis, California 95616*

Fabio Florindo
Leonardo Sagnotti } *Istituto Nazionale di Geofisica, Via di Vigna Murata, 605, I-00143 Rome, Italy*

ABSTRACT

In 1986, cores were obtained to a depth of 702 m (with 98% recovery) from the CIROS-1 drill hole beneath the Ross Sea on the Victoria Land margin. Glaciogene sediments identified near the base of the hole mark the earliest known record of Antarctic glaciation. Initial biostratigraphic analysis indicated that the lower 336 m of the core is early Oligocene in age, and that the upper 366 m is of late Oligocene–early Miocene age. Recently, the chronology of the CIROS-1 core has been questioned. We developed a magnetostratigraphy for the lower 400 m of the CIROS-1 core to clarify the chronology. Our magnetobiostratigraphic results indicate that the base of the CIROS-1 core is early-late Eocene in age (corresponding to Chron C16r; ca. 36.5 Ma). We identify the Eocene-Oligocene boundary at about 410–420 m, within a 20-m-thick, poorly stratified, bioturbated sandy mudstone. This makes the CIROS-1 core the highest latitude site (77.1°S) from which this datum event has been recognized. At 366 m, a 4 m.y. hiatus, which lies immediately beneath fluvial sediments, accounts for most of Chrons C11 and C12. We recognize three major climatic episodes in the CIROS-1 core: (1) the late Eocene (34.5–36.5 Ma, 430–702 m), when relatively warm conditions dominated and there were high sedimentation rates and some glacial activity; (2) the late Eocene–early Oligocene boundary interval (28.5–34.5 Ma, 340–430 m), which was a transition from relatively warm to cooler conditions that coincided with glacial intensification, sea-level fall, and subaerial erosion of the shelf; and; (3) the late Oligocene–early Miocene (22–28.5 Ma, 50–340 m), when large-scale glaciation dominated the region and glaciers grounded across the continental shelf. From correlation with global oxygen isotope and sea-level records, we infer that the Antarctic climate and surrounding oceans cooled after separation of Australia and Antarctica and development of deep-water circulation between them. This marked the onset of the Eocene–Oligocene transition at ca. 34.5 Ma. A major East Antarctic ice sheet did not develop until the early-late Oligocene boundary, toward the end of the Eocene–Oligocene transition (ca. 28.5 Ma). Outlet glaciers did not breach the Transantarctic Mountains and ground across the Ross Sea Shelf until 0.5 m.y. later (ca. 28 Ma).

INTRODUCTION

The timing and style of Antarctic glaciation and its impact on global sea level has been a long-standing issue in Cenozoic paleoceanography. The problem has been compounded by the remoteness of the Antarctic continent and by the scarcity and incompleteness of records from the continent and nearby shelf environments. Kennett (1977) proposed a model for the evolution of Antarctic glaciation that linked the stepwise progression of Southern Ocean $\delta^{18}O$ data (Shackleton and Kennett, 1975) to major events in the tectonic evolution of Antarctica. Kennett (1977) recognized the importance of the separation of Antarctica and Australia but suggested that deep circum-Antarctic flow did not develop until after the opening of the Drake Passage, which was thought to have occurred in the earliest Miocene. Kennett (1977) also concluded that while widespread glaciation probably occurred throughout the Oligocene and early Miocene, the East Antarctic ice cap did not form until the middle Miocene (ca. 14 Ma), after continued isolation of the continent. More recently, Lawver et al. (1992) suggested that the separation of Antarctica and Australia began as early as the Late Cretaceous (ca. 83 Ma), but that major Southern Ocean circulation was probably delayed until the South Tasman Rise finally separated from Antarctica in the late Eocene (ca. 40 Ma) (Fig. 1). Lawver et al. (1992) also suggested that the Drake Passage opened in the early Oligocene (ca. 30 Ma).

As early as 1973, during Leg 28 of the Deep Sea Drilling Project (DSDP), glaciomarine sediment of Oligocene age was recovered from the Ross Sea at DSDP Site 270 (Fig. 1; Hayes et al., 1975). However, discontinuous core recovery and distance from East Antarctica made it difficult to determine the history of the East Antarctic ice sheet. Drilling associated with the McMurdo Sound Sediment and Tectonic Studies (MSSTS) and Cenozoic Investigations in the Ross Sea (CIROS) programs (Barrett et al., 1987, 1989) provided the first continuous stratigraphic evidence from the Antarctic continental margin of the Oligocene–Miocene evolution of the Antarctic cryosphere, including direct evidence of glac-

*Present address: Institute of Geological and Nuclear Sciences, P.O. Box 30368, Lower Hutt, New Zealand; e-mail: wilsongs@geology.ohio-state.edu.

GSA Bulletin; January 1998; v. 110; no. 1; p. 35–47; 8 figures; 1 table.

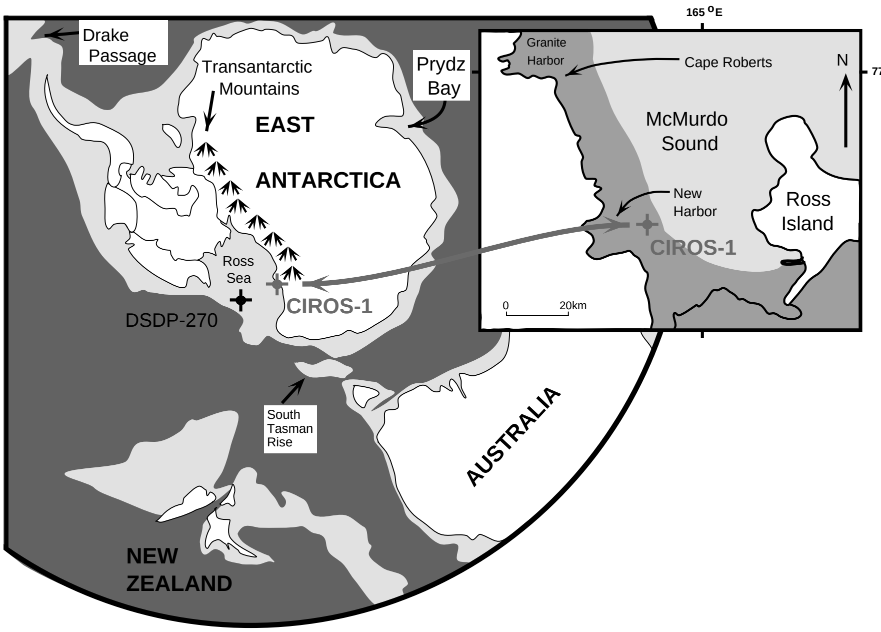

Figure 1. Location of the CIROS-1 drill site (see inset), with paleogeographic reconstruction of southern Gondwana for late Eocene time (after Lawver et al., 1992) around the time of deposition of the basal sediments in the CIROS-1 core. Shaded areas (light gray for map; medium gray for inset) indicate continental margins.

iers grounding beneath sea level on the Ross Sea shelf in Oligocene time. Interpretation of intermediate-resolution seismic reflection data has confirmed that the shelf was deeply scoured by grounding ice sheets by late Oligocene time (Anderson and Bartek, 1992). However, it was not until 1988, with the discovery of Oligocene, and possibly Eocene, glaciogene sediments in Prydz Bay during Leg 119 of the Ocean Drilling Program (ODP), that the existence of continent-wide glacial activity in the Oligocene was confirmed (Barron et al., 1991).

The extent and timing of the onset of Antarctic glaciation clearly have important implications for the paleoclimatology and paleogeography of the Paleogene. Global syntheses indicate that the Paleogene was a time of transition from the uniformly warm climate of the Late Cretaceous to the cooler, more heterogeneous, climate of the Neogene. Berggren and Prothero (1992), in reviewing the available data, concluded that middle Eocene to early Oligocene time was marked by major global climate change and by reorganization of global ocean circulation patterns, coincident with significant turnovers in the marine and terrestrial biota. The transition occurred gradually over at least 10 m.y.; the pattern seems to be one of sequential global extinctions superposed on a gradually cooling earth. The middle–late Eocene has the largest extinction toward the base of Chron C17n.1, which was followed by major cooling and smaller extinction events across the Eocene-Oligocene boundary and in the earliest Oligocene (Berggren and Prothero, 1992).

The CIROS program (Barrett, 1989) has played a major role in attempts to understand the history of Antarctic glaciation. What was originally thought to be an early Oligocene through early Miocene record of sedimentation in the Victoria Land basin was obtained from beneath the southwestern edge of the Ross Sea in the CIROS-1 core (Harwood et al., 1989). The proximity of the CIROS-1 core (lat 77°04.9′S, long 164°29.9′E) to the East Antarctic craton allowed interpretation of terrestrial influences (glacial advances, palynomorphs, and the occurrence of a leaf fossil) within a relatively continuously deposited marine sequence that could be subjected to magnetobiostratigraphic analyses. The data indicate that glaciers grounded across parts of the continental shelf at the same time that cool temperate forests were still extant on the continent (Barrett et al., 1989). This demonstrated that Antarctic glacial history was both more long-lived and more complex than had been previously suggested.

The chronology for CIROS-1 was originally provided by biostratigraphy, by magnetostratigraphy for the upper 360 m (Rieck, 1989), and by a single strontium isotope ratio from a shell near the base of the hole (Barrera, 1989). The sediments were reported to span the interval from the early Oligocene (or possibly latest Eocene) to the early Miocene (ca. 36 to ca. 22 Ma), with a major disconformity between ca. 34.5 and ca. 30.5 Ma at a depth of 366 m (Harwood et al., 1989).

Recently, Hannah (1994) restudied the dinoflagellate stratigraphy of the core and challenged the existing integrated biostratigraphy. He noted that the dinocyst assemblage was environmentally controlled and was therefore unlikely to be reworked, as Harwood et al. (1989) had suggested. Hannah (1994) concluded that the base of the core was middle Eocene in age and that much of the lower part of the core was also Eocene in age. This revision was adopted by Hambrey and Barrett (1994), Barrett et al. (1995), and Bartek et al. (1996). As a result of a new study of the clay mineralogy of the CIROS-1 core, Ehrmann (1997), also concluded that the lower part of the core may be Eocene in age. This conclusion is based on a reduction in smectite concentration and crystallinity at about 420–430 m in the CIROS-1 core. Similar transitions in DSDP and ODP sites from the Southern Ocean have been shown to be coincident with the Eocene-Oligocene boundary (Ehrmann and Mackensen, 1992, Ehrmann et al., 1992).

In this study, we use magnetostratigraphy to resolve the disagreement between different interpretations of the chronology of the CIROS-1 core, particularly for the lower 336 m of the core. Our new chronology is integrated with published biostratigraphic results that are interpreted in the light of recent revisions to Southern Ocean biostratigraphy as well as with redefinitions of global Paleogene chronostratigraphy. We then explore the implications of our synthesis for Antarctic glacial history.

LITHOSTRATIGRAPHY OF THE CIROS-1 CORE

The CIROS-1 core was drilled in 197 m of water beneath McMurdo Sound (Fig. 1) and penetrated to a depth of 702 m below sea floor, with 98% core recovery. Drilling was conducted from a sea-ice platform during October and November 1986 (Barrett, 1987). Hambrey et al. (1989) subdivided the recovered strata into 22 units on the basis of lithofacies (Fig. 2).

The upper sequence (units 1 to 17; 0–366 m) is dominated by glaciogene lithofacies. Hambrey et al. (1989) recognized evidence for at least seven major glacial advances that are marked by thick, massive to weakly stratified diamictites (lodgment and waterlain tills). The lower sequence (units 18–22; 366–702 m) is markedly different in character. It is dominated by alternating fine-grained mudstones and sandstones that are characteristic of relatively deep water and offshore continental shelf settings, with intermittent glacial influence that is far less prominent than in the upper sequence (Hambrey et al., 1989). Dropstones

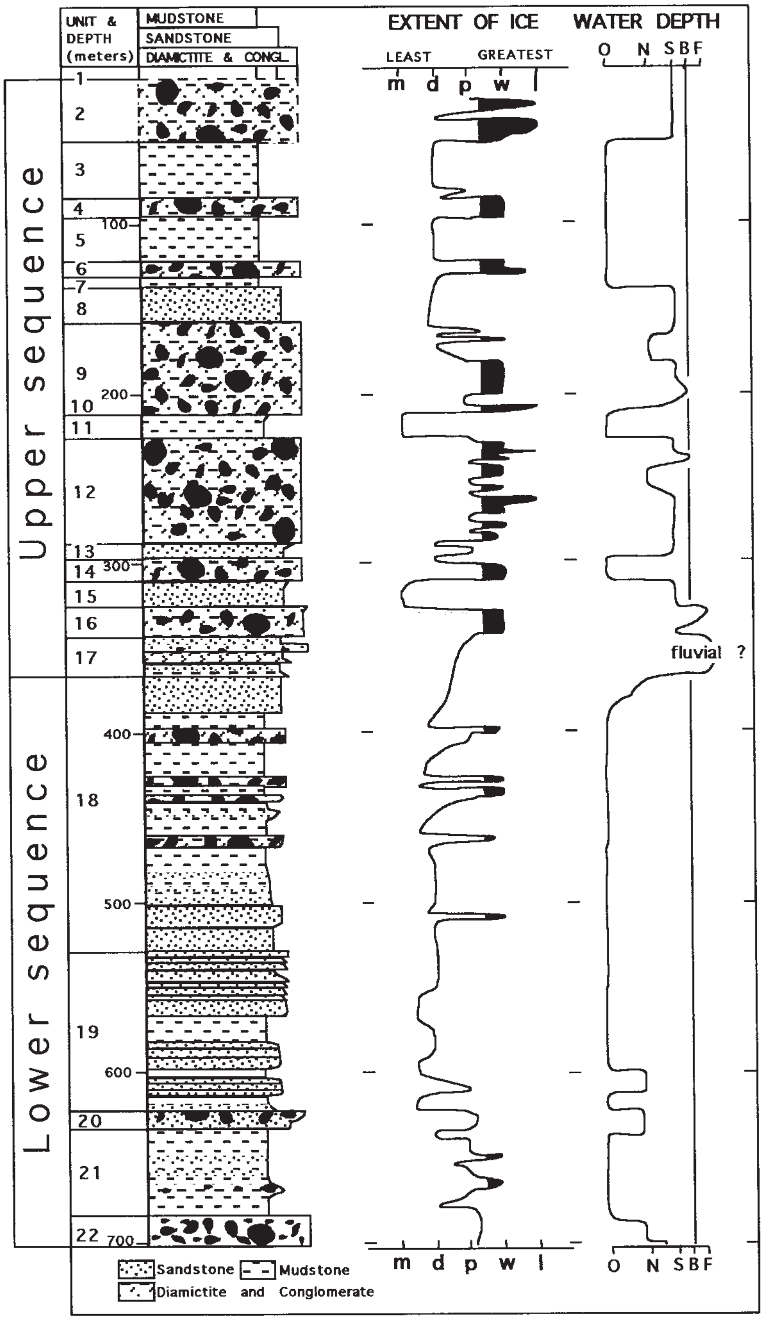

Figure 2. Summary of the lithology of the CIROS-1 core with interpretation of extent of ice and water depth at the CIROS-1 site (after Hambrey et al., 1989). Ice front position: m—marine, d—distal, p—proximal, w—waterlain till, l—lodgment till. Water depth: O—offshore, N—nearshore, S—shoreface, B—beach, F—fluvial. Unit numbers are discussed in the text.

are scattered throughout, which indicates more or less continuous deposition from floating ice. Unit 18 (366–529 m) consists of alternating bioturbated mudstone and sandstone, and minor stratified diamictite. These are interpreted to represent distal shelf sedimentation that was influenced occasionally by floating glacier tongues. Unit 19 (527–624 m) comprises alternating sandstones and mudstones. In general, the sandstone beds are relatively thick (up to 1 m) and massive, and they fine upward into thin mudstone horizons. Rare dropstones are present throughout. Unit 19 is interpreted to represent a succession of sediment gravity flows deposited against a background of quiet sedimentation in a prodelta environment. Toward the base of the lower sequence, two intervals of massive to weakly stratified sandy conglomerate and sand, with rounded and striated clasts (unit 20, 623–634 m, and unit 22, 686–702 m) are interpreted to be debris flow deposits that are indicative of a nearby glacial margin. Also, within unit 21 (634–686 m), Hambrey et al. (1989) recognized an interval of stratified diamictite, which they interpreted to have been deposited by a floating glacier above the CIROS-1 site.

PALEOMAGNETIC METHODS

Sampling

Paleomagnetic samples were obtained from the lower 336 m of the CIROS-1 core at the Antarctic Marine Geology Research Facility at Florida State University in Tallahassee. Since recovery, half of the core has been stored at Florida State University and has been maintained at a constant temperature of 2 °C. The core is in relatively good condition despite considerable drying. Conventional paleomagnetic samples (25 mm diameter) were drilled from the center of the CIROS-1 core and were oriented with respect to vertical (i.e., the up-core direction). Because the core was recovered with a rotary drill, azimuthal orientations were not preserved, and paleomagnetic declinations are arbitrary.

Except for the interval between 623 and 634 m, and below 697 m, samples were taken at an average stratigraphic interval of about 1.6 m, where the sediment texture was suitably fine grained for paleomagnetic analysis. On the basis of existing studies (e.g., Harwood et al., 1989; Wei, 1992; Hannah, 1994), we expected that the maximum age range of the lower 336 m of the core would be from middle Eocene to early Oligocene. Our sampling strategy was designed to produce, at most, an average sampling interval of ~50 k.y., which would probably detect any short polarity intervals. Of the 154 horizons sampled, duplicate samples were taken from 40 horizons to allow comparison of the behavior during thermal and alternating field (AF) demagnetization.

Laboratory Procedures

Paleomagnetic measurements were made at either the University of California at Davis (Davis) or at the Istituto Nazionale di Geofisica (Rome). At Davis, samples were measured on a 2G Enterprises cryogenic magnetometer. For stepwise thermal demagnetization studies, heating was carried out at 20 °C, 80 °C, and then at 40 °C steps to a maximum temperature of 640 °C. Magnetic susceptibility was measured between each heating step to monitor for chemical alteration. Further demagnetization was halted if either the remanence intensity dropped to below the noise level of the magnetometer or if changes in magnetic susceptibility indicated that chemical alteration had occurred. For stepwise AF demagnetization studies, peak fields were set at 5 mT increments to 30 mT and then at 10 mT steps to a maximum peak field of 60 mT. At Rome, samples were measured using a Geofyzika Brno JR-5A spinner magnetometer. For thermal demagnetization studies, heating was carried out at 20 °C, 120 °C, and then at 40 °C steps to 300 °C, then at 330 °C, 360 °C, 400 °C, 450 °C, 500 °C, 540 °C, 580 °C, and 610 °C, with the same procedures for the measurements as those used at Davis. Stepwise AF demagnetization was carried out at the same steps as at Davis.

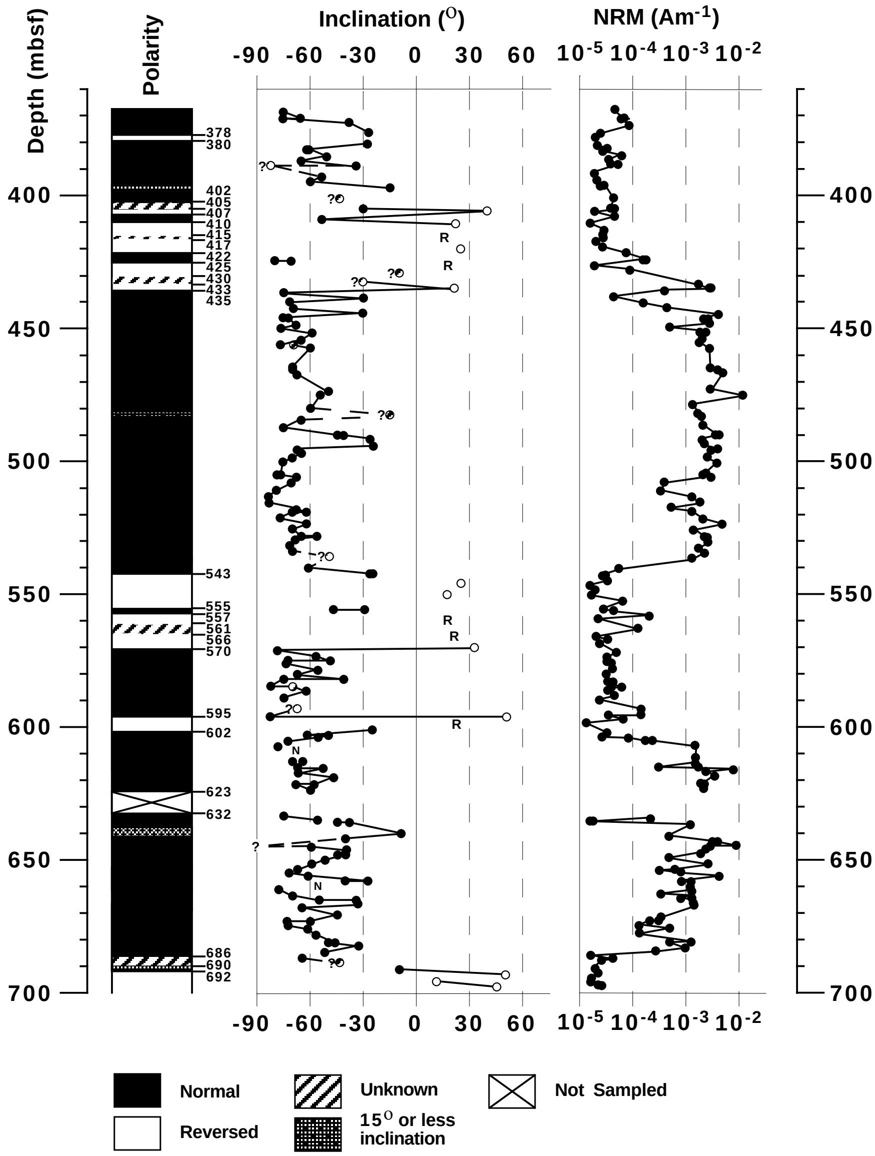

Figure 3. Log of magnetic polarity zonation (black—normal, white—reversed), inclination, and normal remanent magnetization intensities for the lower section of the CIROS-1 core. R (N) denotes samples that displayed a clear trend toward reversed (normal) polarity, but for which a stable characteristic component was not isolated before the remanence fell below the detection limit of the magnetometer.

RESULTS

Paleomagnetic Behavior

Natural remanent magnetization (NRM) intensities for the CIROS-1 core varied widely between 10^{-2} and 10^{-5} Am^{-1} (Fig. 3). Samples from below 685 m, between 540 and 600 m, and above 430 m had weak NRM intensities (<10^{-4} Am^{-1}), while samples between 430 and 540 m and between 600 and 685 m had consistently stronger NRM intensities (>10^{-4} Am^{-1}; Fig. 3). Rieck (1989) also noted this distinct pattern in NRM intensity, although he did not conduct demagnetization experiments or obtain a magnetostratigraphy for the lower 350 m of the CIROS-1 core.

As an interlaboratory comparison, paired samples were measured in both laboratories (Davis and Rome). For magnetized samples that were stable, there was excellent agreement, with paleomagnetic directions differing by a few degrees at most. Another set of paired samples was used to assess whether thermal or AF demagnetization (e.g., Fig. 4b) was the most appropriate method for routine analysis. For samples with NRM intensities above $10^{-3}Am^{-1}$, both demagnetization techniques produced unambiguous paleomagnetic directions that were in close agreement (e.g., Fig. 4a). The remaining samples with NRM intensities above $10^{-3}Am^{-1}$ were then subjected only to AF demagnetization. For samples with moderate NRM intensities (5×10^{-5} to $10^{-3}Am^{-1}$), thermal demagnetization was usually more effective in removing secondary overprints and in isolating a characteristic remanence component (Fig. 4c). The remaining samples with NRM intensities in this range were subjected to thermal demagnetization (e.g., Fig. 4, d–f). Isolation of a characteristic remanence direction for samples with weak NRM intensities (<5×10^{-5} Am^{-1}) was difficult with either demagnetization method.

Most of the samples displayed a low coercivity or low unblocking temperature near-vertical, normal polarity component that is interpreted to represent a drilling-induced overprint (Fig. 4, a–e, h–j). The overprint was usually removed with peak fields of 20–30 mT, or by heating to 250–350 °C. In a few cases, where sample NRM was weak, the drilling-induced overprint could not be removed by either method of demagnetization (Fig. 4e). The ambient geomagnetic field at the site latitude (77°05′S) is also dominated by a vertical component; however, for most samples, stable characteristic remanence directions are easily discernible from the near-vertical drilling-induced overprint (Fig. 4, b, c, h, and i).

For 70% of the samples, stable paleomagnetic behavior was evident in the vector component diagrams, with characteristic remanence directions that generally tended toward the origin. In each of these cases, the primary remanence direction was determined using a best-fit line that was constrained through the origin of the vector component diagram (Fig. 4, b, c, g, and h). For a

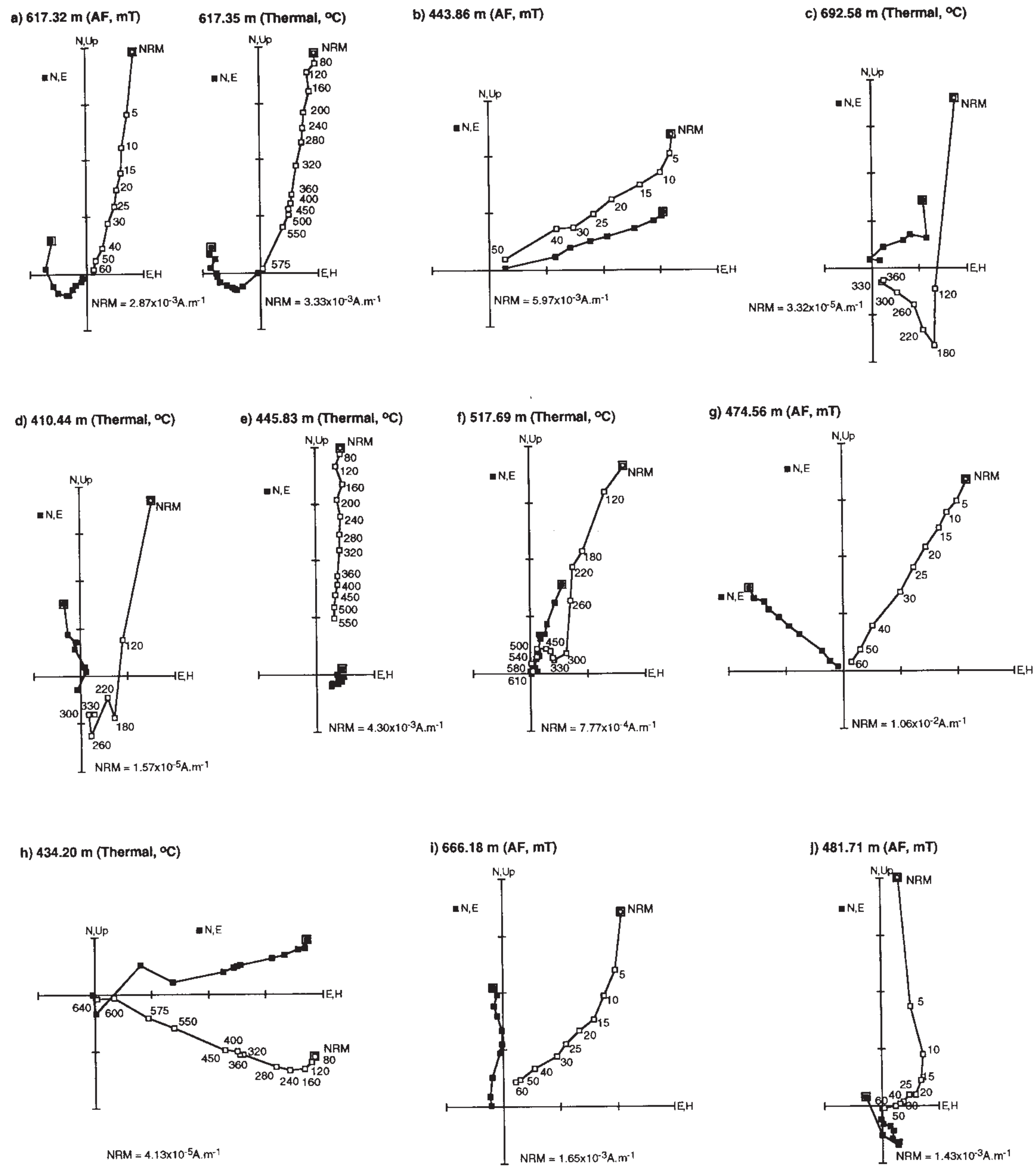

Figure 4. Examples of demagnetization behavior on vector component diagrams of samples from the CIROS-1 core. (a) Comparison of thermal and alternating field demagnetization of normal polarity samples 617.32 and 617.35 m. (b) Normal polarity sample from 443.86 m. (c) Reversed polarity sample from 692.58 m. (d) Reversed polarity sample from 410.44 m. (e) Sample dominated by a drilling-induced overprint at 445.83 m. (f) Normal polarity sample from 517.69 m. (g) Normal polarity sample from 474.56 m. (h) Reversed polarity sample from 434.20 m. (i) Normal polarity sample from 666.18 m. (j) Low inclination normal polarity sample from 481.71 m. Black squares denote projections onto the horizontal plane. White squares denote projections onto the vertical plane.

further 7% of the samples, the characteristic remanence directions did not tend toward the origin and were determined using a best-fit line that was not constrained through the origin (Fig. 4i). It was not possible to determine a clear characteristic direction for the remaining 23% of the samples. Of these, 7% were weakly magnetized samples that had such steep inclinations that we assumed that the drilling-induced overprint was not removed by demagnetization (Fig. 4e). An additional 6% of the samples were weakly magnetized and exhibited no systematic behavior during demagnetization. For the remaining 10% of the samples, stable characteristic remanence directions were not isolated, but the polarity could be inferred by the trend exhibited during demagnetization (e.g., Fig. 4d).

Sagnotti et al. (1996) studied a variety of magnetic properties of the same samples, including anhysteretic remanent magnetization, isothermal remanent magnetization, anisotropy of magnetic susceptibility, thermomagnetic behavior and hysteresis parameters. Several lines of evidence point to magnetite as the primary remanence carrier, including attainment of saturation near 300 mT and maximum unblocking temperatures between 550–600 °C. Temperature-dependent susceptibility measurements contain a major decrease in susceptibility at about 580 °C (Fig. 5), which is also indicative of the dominance of magnetite. Hysteresis measurements indicate that the ratio of saturation remanence to saturation magnetization (M_{rs}/M_s) and of coercivity of remanence to coercive force (H_{cr}/H_c) are within the range of values expected for pseudo-single domain (PSD) magnetite (cf. Day et al., 1977). Sagnotti et al. (1996) concluded that the primary magnetic carrier is PSD magnetite and that the mineralogy is relatively constant throughout the core, with only slight variations in grain-size.

In addition, the magnetic properties and the NRM intensities display a strong stratigraphic affinity that is probably controlled by environmental factors (Sagnotti et al., 1996). In particular, for the intervals from 370 to 430, 540 to 600, and 690 to 700 m, all samples have weak NRM intensity (Fig. 3), low saturation remanence and saturation magnetization, low susceptibility, and a small degree of anisotropy of magnetic susceptibility. These samples exhibit variable and often scattered demagnetization behavior, and their characteristic remanence directions are often difficult to discern. For the intervals from 430 to 540 m and 600 to 690 m, samples have strong NRM intensity (Fig. 3), high saturation remanence and saturation magnetization, high susceptibility, and a high degree of anisotropy of magnetic susceptibility. These samples are paleomagnetically well behaved and are stably magnetized, with characteristic remanence directions that can easily be determined using either AF or thermal demagnetization. There is a slight variation of magnetite grain size between the zones outlined above; however, the major variations in NRM intensity and magnetic properties are probably due to variations in the magnetite concentration. When magnetite is abundant, NRM intensities are strong, and samples are well behaved. When magnetite concentration is low, the paramagnetic clay fraction dominates the magnetic susceptibility, NRM intensities are weak, demagnetization behavior is complex, and reliable characteristic remanence directions are often difficult to determine.

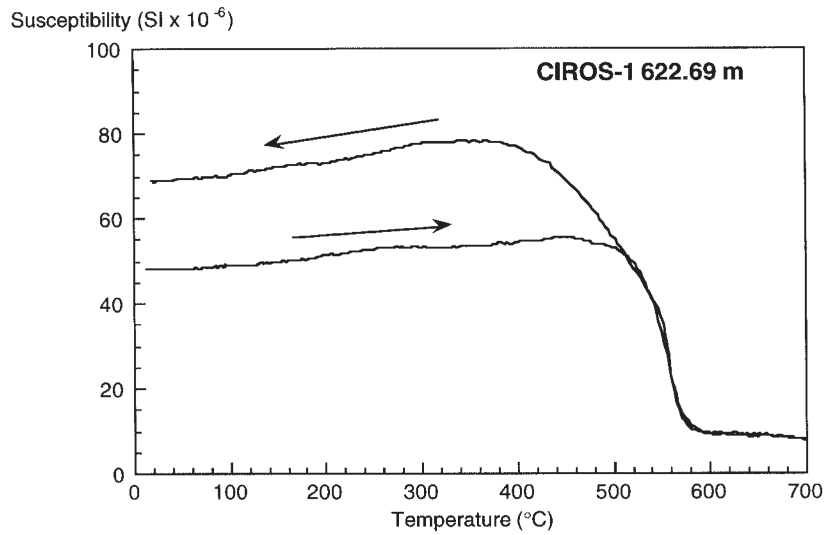

Figure 5. Temperature-dependent susceptibility data for sample from 622.69 m in the CIROS-1 core. The major decrease in susceptibility at 580 °C is indicative of the dominance of magnetite.

MAGNETIC POLARITY STRATIGRAPHY OF THE CIROS-1 CORE

A magnetic polarity stratigraphy for the upper part of the CIROS-1 core (50–350 m) was obtained by Rieck (1989). Our magnetic polarity zonation for the lower part of the core (369–697 m) is shown in Figure 3. This entire interval is below the unconformity that was reported at 366 m and that was interpreted to be ~4 m.y. in duration (Harwood et al., 1989). Two short stratigraphic intervals, from 623 to 632 m and from 697 m to the base of the hole at 702 m, were not sampled because they contain only coarse-grained sediments (Fig. 2) that are unsuitable for paleomagnetic study. Normal polarity dominates the studied interval and accounts for 76% of the lower sequence of the CIROS-1 core. Reversed polarity occurs largely in four distinct intervals that comprise 17% of the strata: 405–435, 543–570, 595–602, and below 692 m (Fig. 3). The remaining 7% of the record has indeterminate polarity.

For many of the reversed polarity samples, the drilling-induced, normal polarity overprint made it difficult to isolate a stable characteristic direction. In many cases, the remanence intensity dropped below the detection limit of the magnetometer before an unambiguously reversed polarity component could be isolated. This was particularly a problem in the weakly magnetized intervals. Despite this difficulty, for many samples there was clearly a trend during demagnetization toward reversed polarity. Such samples are denoted by an R in Figure 3. Correlation of the magnetic polarity zonation with the geomagnetic polarity time scale (GPTS) is discussed below, after the relevant biostratigraphic data are presented.

BIOSTRATIGRAPHIC DATUM EVENTS IN THE CIROS-1 CORE

Calcareous Nannofossils

Edwards and Waghorn (1989) first studied the occurrences of calcareous nannofossils in the CIROS-1 core. They recognized the presence of significant nannofossil assemblages below 385 m, which they considered to be in situ and dominated by reticulofenestrids, with notable occurrences of *Cyclicargolithus floridanus* below 500 m, *Chiasmolithus altus* between 385 and 389 m, *Braarudosphaera bigelowi* between 389 and 684 m, and

Isthmolithus recurvus in a single sample at 417 m. Wei (1992) undertook a more detailed examination of the distribution of calcareous nannofossils below 380 m. He identified three nannofossil zones using the high-latitude zonation of Wei and Wise (1990). Wei (1992) assigned the assemblage recovered from between 392 and 681 m to the *I. recurvus–Blackites spinosus* zones (base = first occurrence datum [FO] of *I. recurvus*, and top = last occurrence datum [LO] of *I. recurvus*), the assemblage recovered from a single sample at 392 m to the *Reticulofenestra daviesii* zone (base = LO *I. recurvus*, top = LO *Reticulofenestra umbilica*), and the assemblage found between 380 and 392 m to the *Chiasmolithus altus* zone (base = LO *R. umbilica*).

In a compilation of the magnetobiostratigraphic data involving *I. recurvus* from Italian type localities and key ODP sites (Fig. 6), Wei (1992) recognized that the LO of *I. recurvus* and, hence, the top of the *Blackites spinosus* zone and base of the *R. daviesii* zone occurred in the lower part of Chron C12r and that the FO of *I. recurvus* at high southern latitude ODP sites occurred within Chron C16n.2n. However, the LO of *I. recurvus* is more variable in lower latitude localities, sometimes occurring earlier, within Chron C13n.

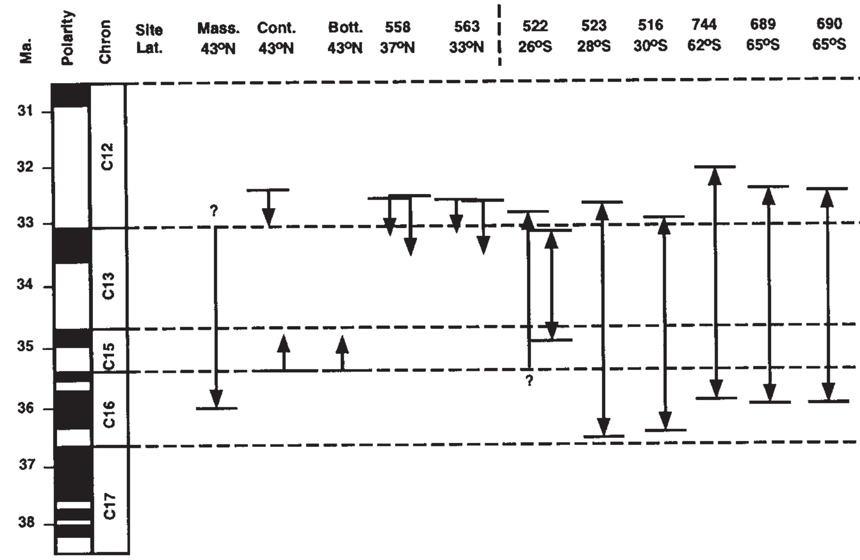

Figure 6. Compilation of global magnetobiostratigraphic data for *Isthmolithus recurvus* (modified from Wei, 1992). Mass.—Massignano, Italy (Coccioni et al., 1988); Cont.—Contessa, Italy (Monechi and Theirstein, 1985); Bott.—Bottaccione, Italy (Lowrie et al., 1982). Numbers refer to Deep Sea Drilling Project–Ocean Drilling Program sites, and were referenced by Wei (1992). The chronostratigraphy is from Cande and Kent (1992, 1995) and Berggren et al. (1995).

Marine Diatoms

Harwood et al. (1989) identified marine diatoms as potentially the best microfossil group for establishing age control for the CIROS-1 core. Harwood (1989) identified three distinct siliceous microfossil biostratigraphic zones: assemblage zone C (702–502 m), which contains extremely poorly preserved early Oligocene assemblages, including common silicified casts of diatoms (*Liostephania*); assemblage zone B (500–367 m), which contains rich, well-preserved early Oligocene assemblages; and assemblage zone A (366–27 m), which contains moderately well-preserved late Oligocene to early Miocene assemblages that had previously been identified from the nearby MSSTS-1 core (Harwood, 1986). It is important to note that the early Oligocene age of assemblage zones B and C was based on the time scale of Berggren et al. (1985); the revised time scale of Berggren et al. (1995) puts this interval within the late Eocene–early Oligocene. The only clear evidence for glacial reworking in the CIROS-1 core is the occasional up-core occurrence of the more resistant *Liostephania*, which appear to be derived from an assemblage similar to that found below 500 m. Otherwise, all occurrences of siliceous microfossils are believed to be in situ.

Key datum events in the CIROS-1 core from below 300 m, with locations and ages identified by Harwood and Maruyama (1992), include FO *Hemiaulus caracteristicus* (645 m; C17n.1n), FO *Asterolampra punctifera* (500 m; C13r/C15n), FO *Stephanopyxis splendidus* (syn. *Thalassiosira hydra*; 500 m; C15n), FO *Eurossia irregularis* (syn. *Triceratium polymorphus*; 500 m; C15n), FO *Rhizosolenia oligocenica* (syn. *R. gravida*; 438 m; C13r/C15n or older), LO *R. oligocenica* (383 m; near the top of C12r), LO *Sphinctolethus pacificus* (383 m; C11n.2n), LO *H. caracteristicus* (375 m; C11n.2n), FO *Synedra jouseana* (360 m; C12n), and LO consistent *Pyxilla reticulata* (367 m; C12n).

Foraminifera

Webb (1989) identified several low-diversity foraminiferal assemblages from the CIROS-1 core. He found these to be mostly in situ, but not highly age diagnostic. Below 366 m, Webb (1989) recognized two assemblages that exhibit close affinities with Eocene-Oligocene cosmopolitan bathyal-abyssal assemblages that are commonly encountered in lower latitude successions at drill sites in the southwest Pacific and Atlantic Oceans.

Below 690 m, Webb (1989) recognized the Eocene planktonic foraminifera *Pseudoglobo-quadrina primativa* (LO C16r; Jenkins, 1985; Edwards et al., 1989), and below 668.78 m, he found benthic taxa (*Nonion* cf. *graniferum* and *Alabamina dissonata*), which are restricted to the Eocene. However, because of uncertainty in their stratigraphic ranges, Webb (1989) was not convinced that the strata from which they were recovered were of Eocene age. Webb (1989) also identified the FO of *Epistominella exigua* in the CIROS-1 core at 497 m and, more recently, R. Coccioni and S. Monechi (1996, personal commun.) reported this datum event at a depth of 558 m. This was suggested to be a post-Eocene form by Wood et al. (1985); however, it is a benthic form with strong environmental affinities, which suggests its occurrence is not strongly age diagnostic (P.-N. Webb, 1996, personal commun.).

Marine Palynomorphs

Wilson (1989) reported a low-diversity palynoflora from beneath 473 m in the CIROS-1 core. These assemblages comprise a distinctive high-latitude suite that was first described from surficial erratics in the McMurdo Sound area and was assigned to the Eocene–Oligocene by Wilson (1967) and Wilson and Clowes (1982). Key forms include *Arachnodinium antarcticum*, *Alterbidinium distinctum*, *Areosphaeridium* cf. *dictyoplokus* (syn. *Enneadocysta partridgei*; reported to range from the Bartonian [C19] through the Rupelian [C10] by Stover and Williams, 1995), *Deflandrea antarctica* (reported to range from the Eocene to the early-late Oligocene boundary by Mohr, 1990), *Spinidinium macmurdoense* (reported to range from the Eocene to the mid-Oligocene in New Zealand by Wilson, 1967), *Tubiosphaera filosa* (reported to range into upper Eocene strata by Crouch and Hollis, 1996, with Oligocene occurrences reported by Evitt and Pierce, 1975), and *Vozzhennikovia apertura*. This last assemblage had been assigned a late Eocene age by earlier workers (e.g., McIntyre and Wilson, 1966; Kemp, 1975; Hall, 1977; Goodman and Ford, 1983), but Wilson (1989) reported that it was commonly reworked into Oligocene strata. Wilson (1989) also noted that the relatively common occurrence of *Phthanoperidinium* sp. at 692–696 m is probably in situ and indicates an early Oligocene age, which suggests that many of the Eocene forms may have been reworked.

More recently, Hannah (1994, 1996) recognized several distinctive dinoflagellate zones in the lower half of the CIROS-1 core that were primarily environmentally controlled and which he interpreted to represent in situ and not reworked assemblages, as had been the interpretation of Harwood et al. (1989). Between 455 and 702 m, Hannah (1994) recognized the same key species as Wilson (1989) but used the occurrence of *Hystrichosphaeridium tubiferum* specifically to suggest that this assemblage was restricted to the middle Eocene. However, Goodman and Ford (1983) had reported *H. tubiferum* in late Eocene strata from DSDP Site 511, and other workers have not considered *H. tubiferum* to be stratigraphically diagnostic (e.g., Williams and Bujek, 1985; Wrenn and Hart, 1988). After reconsidering the palynological evidence, Hannah (1996) suggested that the basal interval of the CIROS-1 core was late Eocene rather than middle Eocene in age.

Strontium Isotope Ratio

A single strontium isotope ratio age was obtained from aragonitic shell material found at a depth of 678.71 m in the CIROS-1 core (Barrera, 1989). An $^{87}Sr/^{86}Sr$ ratio of 0.707764 ± 20 with respect to NBS-987 indicates an age between 34 and 36 Ma when compared directly to the strontium isotope curve for sea water given by Miller et al. (1988). After adjusting for the Sr standard used by Miller et al. (1988), Harwood et al. (1989) concluded that the age obtained from near the base of CIROS-1 can be no younger than ca. 34 Ma, due to the flattening of the $^{87}Sr/^{86}Sr$ curve beyond the early Oligocene. It should be noted that Miller et al. (1988) estimated the stratigraphic resolution for the strontium isotope curve in the latest Eocene–Oligocene to be approximately 2 m.y.

CORRELATION WITH THE GEOMAGNETIC POLARITY TIME SCALE

The most reliable biostratigraphic datum events from the lower 350 m of the CIROS-1 core (as discussed above) are summarized in Table 1. The locations and ages of these datum events are used in Figure 7 to construct the shaded time-depth window within which the correlation to the GPTS must fall.

Rieck (1989) conducted AF demagnetization studies of the upper 380 m of the CIROS-1 core and reported a magnetic polarity zonation to 344 m depth. He used biostratigraphic indicators and correlations with the magnetostratigraphy for the MSSTS-1 core to identify Chrons C6 through C10. However, below 344 m in the core, he was not able to reliably determine the polarity using AF techniques. The coarse-grained lithologies between 344 and 366 m depth prevented detailed paleomagnetic sampling of this interval. In Figures 7 and 8, we have shown the polarity interpretations of Rieck (1989) and Harwood et al. (1989) above 344 m depth, our polarity interpretations below 366 m depth, and marked the interval between 344 and 366 m depth as unsampled.

The latest Eocene–early Oligocene is a time of dominantly reversed polarity; however, our new data are predominantly of normal polarity. This suggests that a substantial portion of the CIROS-1 core below the unconformity at 366 m was not deposited during the early Oligocene and latest Eocene (Chrons C12 and C13) but during the middle to late Eocene, which is a time of dominantly normal polarity (Chrons C15 through C17). This inference is consistent with the time-depth window shown in Figure 7.

A more refined correlation to the GPTS can be obtained by considering certain key biostratigraphic datum events. One of the most important and reliable of these is the range of the calcareous nannofossil *I. recurvus*. As noted above, Wei (1992) demonstrated that at high southern latitudes, the FO of this datum event always occurs within Chron C16n.2n (Figs. 6 and 7). In the CIROS-1 core, this FO (N2) is found at 681 m. We therefore correlate the reverse-normal (R-N) polarity transition at 692 m with the base of Chron C16n.2n (Fig. 7). The LO of *Pseudogloboquadrina primativa* (F1) at 690 m is consistent with this correlation.

At 500 m, we note the common FOs of *A. punctifera* and *S. splendidus* (D1), both of which occur within Chron C13r or C15n. We therefore correlate the reverse-normal polarity transition at 543 m with the base of Chron C15n, and the underlying normal polarity interval between 570 and 595 m with Chron C16n.1n (Fig. 7). At 392 m, we recognize the LO of *I. recurvus* (N1). Wei (1992) has shown that this datum event occurs just above the base of Chron C12r. In the CIROS-1 core, this datum event lies in a normal polarity interval that extends from 380 to 405 m. We therefore correlate this interval with Chron C13n (Fig. 7). The LO of *R. oligocenica* (D3) at 383 m is consistent with this correlation. These correlations establish that the Eocene-Oligocene boundary must occur between about 410 and 420 m in the CIROS-1 core.

The FO of *S. jouseana* (D7, C12n) at 360 m suggests that strata above the unconformity identified at 366 m by Hambrey et al. (1989) and Harwood et al. (1989), are of Chron C12n age or younger. Extrapolation from the age depth plot of Rieck (1989) and Harwood et al. (1989) suggests that these strata may well be as young as Chron C10. Immediately beneath the unconformity, the interval of normal polarity extending from 366 to 378 m depth is separated from the underlying normal polarity interval by a single sample of reversed polarity at 379 m. Correlation of this interval of normal polarity with the GPTS is ambiguous. The LO of *P. reticulata* (D6) at 367 m raises the possibility that this normal polarity interval might be correlated with Chron C12n and that most of Chron C12r is missing in an unconformity at ~378 m depth. However, there is no lithologic disconformity at this depth. Higher in the CIROS-1 core, there are multiple disconformities within lithostratigraphic units 16 and 17 (326–366 m). Hambrey et al. (1989) interpreted these to be mostly of terrestrial origin, which suggests prolonged exposure of the continental shelf during this time. It is therefore likely that much time is missing in this interval between 326 and 355 m in the core (and perhaps most of the time is missing in the basal unconformity of unit 17, at 366 m). For this reason, we prefer to correlate the entire normal polarity interval between 366 and 405 m with Chron C13n, and we conclude that at least Chron C12r and probably most of Chrons C10 through C12n are also missing in the unconformity at 366 m (Fig. 7).

On the basis of the above correlation to the GPTS, the average sedimentation rate for the lower 320 m of the CIROS-1 core is about 90 m/m.y. (Chrons C16r through C13n). The unconformity at 366 m depth accounts for at least 2 m.y. and probably as much as 4 m.y. as inferred by Harwood et al. (1989). The average sedimentation rate above the unconformity is about 35 m/m.y.

Our magnetostratigraphic interpretation of the CIROS-1 core raises certain issues that need to be addressed. First, the LO of *I. recurvus* (N1) occurs in Chron C13n. It was expected from the work of Wei (1992) that the LO would be in Chron C12r, although he reports a LO within Chron C13n at DSDP Site 522. Wei (1992) ruled out reworking of *I. recurvus* in CIROS-1 because

TABLE 1. BIOSTRATIGRAPHIC DATA USED TO AID CORRELATION OFTHE CIROS-1 MAGNETIC POLARITY ZONATION WITH THE GEOMAGNETIC POLARITY TIME SCALE

Event	Depth	Datum*	Chron	References
Diatoms				
D1	500 m	FO *Asterolampra punctifera*	C13r/C15n	All diatom datums from Harwood and Maruyama (1992),
		FO *Stephanopyxis splendidus*	C13r/C15n	Harwood (1989), and Harwood et al. (1989), and
D2	438 m	FO *Rhizosolenia oligocaenica*	C13r/C15n or older	references therein.
D3	383 m	LO *Rhizosolenia oligocaenica*	C12	
D4	383 m	LO *Sphynctolethus pacificus*	C11n.2n	
D5	375 m	LO *Hemiaulus caracteristicus*	C11n.2n	
D6	367 m	LO consistent *Pyxilla reticulata*	C12	
D7	360 m	FO *Synedra jouseana*	C12n	
Foraminifera				
F1	690 m	LO *Pseudogloboquadrina primativa*	C16r or poss. younger	Jenkins (1985), Edwards et al. (1989), Harwood et al. (1989), and Webb (1989).
F2	669 m	LO *Nonion* cf. *graniferum*	C13r or older	Datums at 669 m from Harwood et al. (1989), and
		LO *Alabamina dissonata*	C13r or older	Webb (1989).
F3	558 m	FO *Epistominella exigua*	N.D.†	Coccioni and Monechi (1996, personal commun.).
Calcareous nannofossils				
N1	392 m	LO *Isthmolithus recurvus*	C12r	Both datums from Wei (1992), Harwood et al. (1989),
N2	681 m	FO *Isthmolithus recurvus*	C16n.2n	and Edwards and Waghorn (1989).
Marine palynomorphs				
P1	473 m	LO *Arachnodinium antarcticum*	C10/C12	Harwood et al. (1989) and references therein.
P2	455 m	LO *Enneadocysta partridgei*	C10	Datums at 455 m from Brinkhuis (1992), Crouch and
		LO *Deflandrea antarctica*	C10	Hollis (1996), Evitt and Pierce (1975), Hannah (1984 and
		LO *Spinidinium macmurdoense*	C10	1986), Harwood et al. (1989), Kemp (1975), Mohr
		LO *Tubiosphaera filosa*	C10	(1990), Stover and Williams (1995), and Wilson (1967, 1989).
Strontium isotope ratio				
S1	679 m	$^{87}Sr/^{86}Sr$ = 0.707764 ± 20 (NBS-987)	C13n or older	Barrera (1989), Harwood et al. (1989), Miller et al. (1989).

*FO refers to first occurrence datum; LO refers to last occurence datum.
†N.D. = no data available.

the datum co-occurs with other forms. Also, Wei (1992) did not observe any lower Paleogene or Mesozoic forms that had been reworked into the CIROS-1 strata. Given the deterioration of the Antarctic environment during this time interval, it is possible that these nannofossils might have become extinct sooner in the Ross Sea area than elsewhere in the Southern Ocean. Also, the FO of *E. exigua* (F3) occurs near the base of Chron C15 in CIROS-1, which would place it in the Eocene, although Wood et al. (1985) from studies in Barbados had concluded it was a post-Eocene form. However, earlier in this paper, we discussed the environmental affinities of this benthic form and pointed out that it was long ranging and hence not very age diagnostic.

There are several short polarity intervals in our magnetostratigraphic interpretation of the CIROS-1 core that are not observed in the GPTS of Cande and Kent (1992, 1995). These short intervals have stable paleomagnetic directions that are often of low angle, with inclinations <30° and sometimes <15° (see, for example, 493 m in Fig. 3). Similar features have been reported by Turner and Bryant (1995) in Eocene sandstones of the Taranaki basin, New Zealand. As in the study of Turner and Bryant (1995), we find that the short polarity, low inclination intervals are not restricted to specific lithostratigraphic units or to intervals of distinctive paleomagnetic behavior. Some of these features may be attributable to global geomagnetic phenomenon known as *tiny wiggles* (e.g., Cande and Kent, 1992). Lanci et al. (1996) reported detailed magnetostratigraphic results from the Eocene-Oligocene boundary interval in an Italian sequence, where they documented the presence of short normal polarity magnetozones within Chron C16n.1r for which there are no corollaries in the GPTS.

Hartl et al. (1993) and Tauxe and Hartl (1997) reported paleogeomagnetic studies of Oligocene strata recovered from DSDP site 522. Within Chron C12r, they observed nine zones of unusually low relative paleointensity, which they interpreted to correlate to the tiny wiggles reported by Cande and Kent (1992). Hartl et al. (1993) and Tauxe and Hartl (1997) also showed that the zones of low paleointensity are sometimes associated with excursions in a direction that have virtual geomagnetic poles as much as 75° from the geographic pole. Such excursions could have been recorded as nearly fully reversed events at high latitude sites such as that of CIROS-1. Given the high sedimentation rates that we calculate for CIROS-1, it is not surprising to find short polarity events filtered out of the marine magnetic anomaly records from which the GPTS of Cande and Kent (1992, 1995) was derived. We propose that the brief, and often shallow inclination, features that we observe in the CIROS-1 magnetic polarity record are possibly equivalent to the previously unidentified cryptochrons reported by Lanci et al. (1996).

DISCUSSION

From our analysis, we interpret the base of the CIROS-1 core to be early late Eocene in age (ca. 36.5 Ma, using the time scale of Berggren et al., 1995). Harwood et al. (1989) assigned an early Oligocene, possibly latest Eocene, age to the basal CIROS-1 sediments (36 Ma, using the time scale of Berggren et al., 1985), but the redefinition and shifting of age datum events by Berggren et al. (1995) means that although our results indicate an Eocene age for these sediments, our numerical age estimate is almost identical to that given by Harwood et al. (1989). The paleomagnetic results have, however, improved the resolution and dating of other events in the CIROS-1 core, something that was not possible using biostratigraphic methods alone. The basal units in the core, which Hambrey et al. (1989) interpreted to have had been deposited during glaciation of the region, occur within Chron C16n.2n and are also late Eocene in age (ca. 36 Ma). Sedimentation above this was rapid

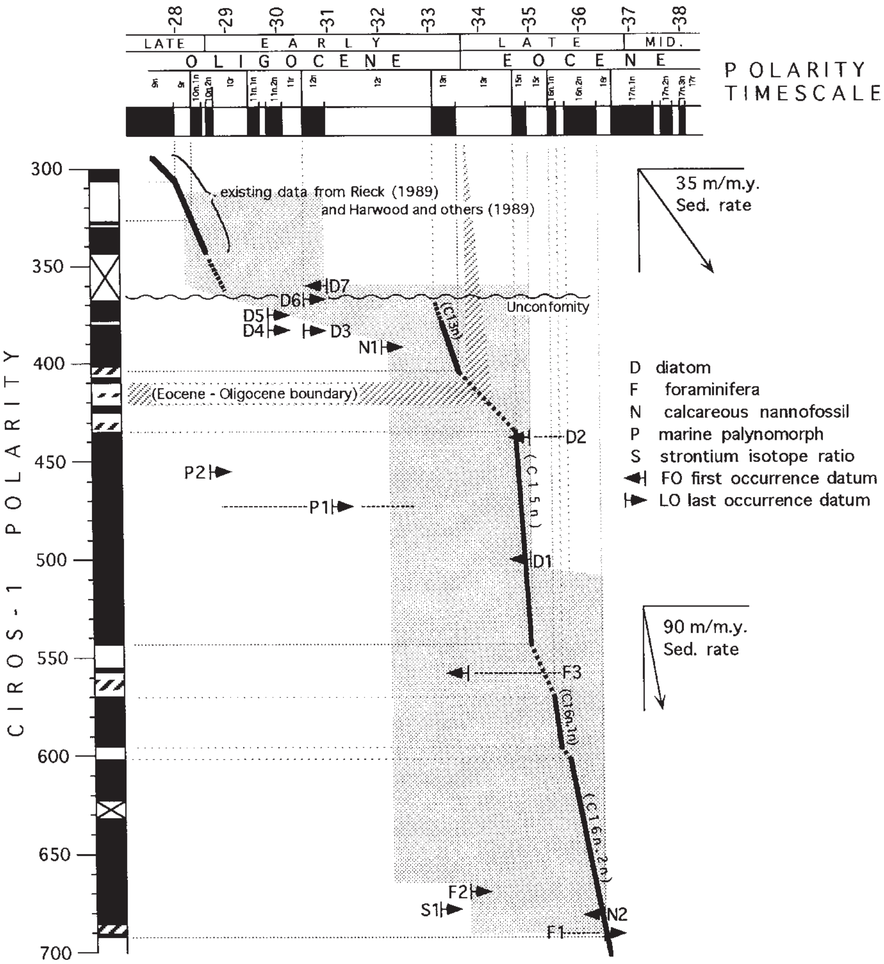

Figure 7. Correlation of the CIROS-1 magnetic polarity zonation with the geomagnetic polarity time scale of Cande and Kent (1992, 1995) and Berggren (1995). Magnetic polarity symbols are defined in Figure 3. Line of correlation: solid—correlation is unambiguous; dashed—correlation is inferred. Continuous stippled lines—important correlation tie points (see discussion in text), dashed stippled lines—secondary correlation tie points. The shaded area is the time-depth window (defined by data discussed in text) within which the correlation to the geomagnetic polarity time scale must fall. Datum events, with alpha-numeric indicators that were used to constrain the correlations, are given in Table 1. See discussion of interpretation in text.

(about 90 m/m.y.) and relatively continuous despite the extensive number of sediment gravity flows that occur in the basal 200 m of the core (Barrett et al., 1989). The hiatus identified at 366 m depth by Hambrey et al. (1989) is 4 m.y. in duration as inferred by Harwood et al. (1989) and accounts for much of Chrons C11 and C12. However, we cannot rule out the possibility that the time is missing in several unconformities between 344 and 366 m.

On the basis of our magnetostratigraphy, the Eocene-Oligocene boundary interval, as defined by Berggren et al. (1995), occurs at about 410–420 m, within a 20-m-thick, poorly stratified, bioturbated, sandy mudstone (Hambrey, 1989). This makes the CIROS-1 core the highest latitude site from which the Eocene-Oligocene boundary has been recognized. The Eocene-Oligocene boundary interval seems to have been preserved in the CIROS-1 core and does not appear to be coincident with an unconformity, as is the case for other sites (Prothero and Berggren, 1992), although we do not have enough data to identify the exact position of the boundary.

On the basis of our new chronology, the facies interpretations of Hambrey et al. (1989), and the environmental interpretations of Barrett (1989), we recognize three major climatic episodes in the CIROS-1 core. The first is the late Eocene (34.5–36.5 Ma, 430–702 m), when relatively warm conditions dominated with rapid sedimentation and some glacial activity. The second is the Eocene–Oligocene boundary interval (28.5–34.5 Ma, 340–430 m) which was a variable transition from relatively stable warm conditions to cooler conditions. This interval has a duration of only ~6 m.y., which is temporally condensed relative to reports of the transition from other parts of the globe (e.g., Prothero and Berggren, 1992). The third is the late Oligocene–early Miocene (22–28.5 Ma, about 50–340 m), when large-scale glaciation dominated the region, with glaciers grounding across the continental shelf.

IMPLICATIONS FOR DEVELOPMENT OF THE ANTARCTIC CRYOSPHERE

The available environmental interpretations for the CIROS-1 core (Hambrey et al., 1989; Barrett, 1989) are summarized in Figure 8. Our magnetostratigraphy enables us to correlate these environmental indicators with global Paleogene events, including the glacioeustatic curve of Haq et al. (1988), the $\delta^{18}O$ curve of Miller (1992), as well as the time scales of Cande and Kent (1992, 1995) and Berggren et al. (1995). Below about 430 m, in late Eocene time, average sedimentation rates were high (about 90 m/m.y.), and the CIROS-1 site was in an outer-shelf setting. By ~0.5 to 1 m.y. prior to the Eocene-Oligocene boundary (of Berggren et al., 1995), at the beginning of the Eocene-Oligocene transition of Prothero and Berggren (1992) and corresponding to a depth of ~430 m, the average rate of sedimentation slowed to less than 10 m/m.y., and the CIROS-1 lithostratigraphy indicates the beginning of glacial intensification, coincident with a major cooling documented by the $\delta^{18}O$ record (Miller, 1992) and by an abrupt increase in cool-water nannofossil taxa in the Southern Ocean (Wei, 1991).

A major faunal change farther down in the CIROS-1 core at 500 m (ca. 35 Ma) is also indicative of substantial cooling, and the Eocene–Oligocene transition may have already begun by this time on the Antarctic shelf. Toward the end of the transition, above 366 m, Barrett (1989) and Hambrey et al. (1989) recognized an extended interval (50 m) of terrestrial sedimentation, with intermittent erosion and subaerial exposure of the Ross Sea shelf at the CIROS-1 site. These events are contemporaneous with the major sea-level fall at the early-late Oligocene boundary (ca. 28.5 Ma), as identified by Haq et al. (1988). These events probably mark the buildup of the first major ice sheet on the Antarctic craton and the end of the

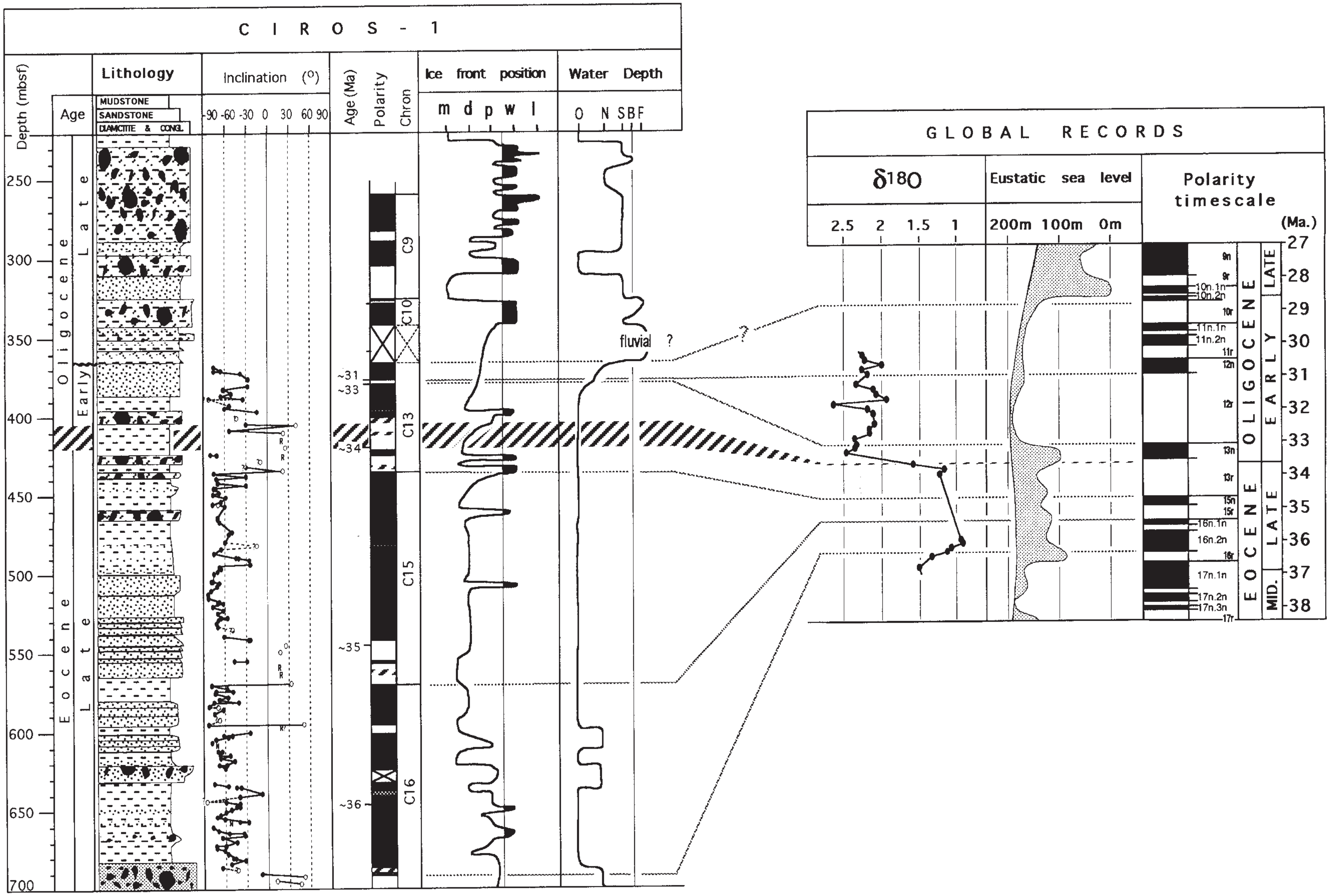

Figure 8. Summary of the new chronology of the CIROS-1 core, including interpreted ice front position and water depth at the CIROS-1 site (from Hambrey et al., 1989), with global Paleogene events, including the $\delta^{18}O$ curve of Miller (1992), the glacioeustatic curve of Haq et al. (1988), and the time scale of Cande and Kent (1992, 1995) and Berggren et al. (1995). See discussion of interpretation in text.

Eocene–Oligocene transition of Prothero and Berggren (1992). However, it was not until 0.5 m.y. later (ca. 28 Ma) that glaciers grounded across the Ross Sea shelf, as recorded by extensive lodgment till in the CIROS-1 core (Hambrey et al., 1989). We suggest that the 0.5 m.y. lag in the appearance of glaciers on the Ross Sea shelf represents the time it took for ice from the East Antarctic ice sheet to flow though the Transantarctic Mountains to the CIROS-1 site. Major ice sheet buildup on the Antarctic craton prior to 28.5 Ma is unlikely because there is no similar major glaciation recorded in the CIROS-1 core that is correlative with the late Eocene (ca. 36.8 Ma) global sea-level fall identified by Haq et al. (1988). Furthermore, pre–late Eocene fluctuations in sea level are less pronounced and are of shorter duration than the late Eocene and late Oligocene events.

We infer the following scenario for the Eocene–Oligocene transition and development of the East Antarctic ice sheet. Following the final separation of Australia and Antarctica and development of deep-water circulation between them (post–ca. 40 Ma; Lawver et al., 1992), the Antarctic climate and surrounding oceans cooled, marking the onset of the Eocene–Oligocene transition at ca. 34.5 Ma. Thermal isolation and the development of a major East Antarctic ice sheet did not occur until the early-late Oligocene boundary, toward the end of the Eocene–Oligocene transition (ca. 28.5 Ma), which was coincident with the major eustatic sea-level fall identified by Haq et al. (1988). Development of the East Antarctic ice sheet may have resulted either from the initial opening of the Drake Passage (ca. 30 Ma; Lawver et al., 1992) and the subsequent development of the circumpolar current, or from early uplift of the Transantarctic Mountains, which provided a physiographic barrier for ice sheet growth (Fitzgerald, 1992). It was not until 0.5 m.y. later that outlet glaciers breached the Transantarctic Mountains and grounded across the Ross Sea Shelf.

The uplift of the Transantarctic Mountains and the role of tectonics in exposing the Antarctic shelf as well as the development of the East Antarctic ice sheet toward the end of the Eocene–Oligocene transition are not well understood. Additional work is necessary to understand the role of glacial activity that is clearly present in the CIROS-1 core (although at a much reduced level) before the early-late Oligocene boundary (before the formation of the East Antarctic ice sheet). The aims of the Cape Roberts Project (Barrett and Davey, 1992; Webb and Wilson, 1994) are to recover an older Paleogene sequence that will lead to further investigation of these questions.

ACKNOWLEDGMENTS

This work was supported by National Science Foundation grants OPP-9522309 and OPP-9526889 to Verosub and Roberts, and grant OPP-9527343 to Wilson. Sagnotti and Florindo acknowledge financial support from PNRA (Italian National Antarctic Research Program). We thank Donald Prothero and John Flynn for reviews, and Matthew Curren and Tom Janecek for assistance with sample collection at the Antarctic Marine Geology Research Facility, Florida State University. Aspects of the biostratigraphy presented here were discussed with Rosemary Askin, Rodolfo Coccioni, David Harwood, Richard Levy, Simonetta Monechi, and Peter Webb. We thank Rodolfo Coccioni and Simonetta Monechi for sharing their new foraminiferal data from the CIROS-1 core; Rosemary Askin, Peter Barrett, David Harwood, and Peter Webb for reviewing an earlier version of the manuscript; and Maria Bianca Cita and Antonio Meloni for their support and encouragement.

REFERENCES CITED

Anderson, J. B., and Bartek, L. R., 1992, Cenozoic glacial history of the Ross Sea revealed by intermediate resolution seismic reflection data combined with drill site information, *in* Kennett, J. P., and Warnke, D. A., eds., The Antarctic paleoenvironment: A Perspective on global change. Part 1: American Geophysical Union Antarctic Research Series, v. 58, p. 231–263.

Barrera, E., 1989, Strontium isotope ages, *in* Barrett, P. J., ed., Antarctic Cenozoic history from the CIROS-1 drillhole, McMurdo Sound, Antarctica: Wellington, New Zealand, DSIR Publishing, Department of Scientific and Industrial Research Bulletin, v. 245, p. 151–152.

Barrett, P. J., ed., 1986, Antarctic Cenozoic history from the MSSTS-1 drillhole, McMurdo Sound, Antarctica: Wellington, New Zealand, DSIR Publishing, Department of Scientific and Industrial Research Bulletin, v. 237, 174 p.

Barrett, P. J., ed., 1989a, Antarctic Cenozoic history from the CIROS-1 drillhole, McMurdo Sound, Antarctica: Wellington, New Zealand, DSIR Publishing, Department of Scientific and Industrial Research Bulletin, v. 245, 254 p.

Barrett, P. J., 1989b, Introduction, *in* Barrett, P. J., ed., Antarctic Cenozoic history from the CIROS-1 drillhole, McMurdo Sound, Antarctica: Wellington, New Zealand, DSIR Publishing, Department of Scientific and Industrial Research Bulletin, v. 245, p. 5–6.

Barrett, P. J., 1989c, Sediment texture, *in* Barrett, P. J., ed., Antarctic Cenozoic history from the CIROS-1 drillhole, McMurdo Sound, Antarctica: Wellington, New Zealand, DSIR Publishing, Department of Scientific and Industrial Research Bulletin, v. 245, p. 49–58.

Barrett, P. J., and Davey, F. J., eds., 1992, Antarctic stratigraphic drilling, Cape Roberts Project, workshop report: Royal Society of New Zealand Miscellaneous Series, v. 23, 38 p.

Barrett, P. J., Elston, D. P., Harwood, D. M., McKelvey, B. C., and Webb, P.-N., 1987, Mid-Cenozoic record of glaciation and sea-level change on the margin of the Victoria Land basin, Antarctica: Geology, v. 15, p. 634–637.

Barrett, P. J., Hambrey, M. J., Harwood, D. M., Pyne, A. R., and Webb, P.-N., 1989, Synthesis, *in* Barrett, P. J., ed., Antarctic Cenozoic history from the CIROS-1 drillhole, McMurdo Sound, Antarctica: Wellington, New Zealand, DSIR Publishing, Department of Scientific and Industrial Research Bulletin, v. 245, p. 241–251.

Barrett, P. J., Henrys, S. A., Bartek, L. R., Brancolini, G., Busetti, M., Davey, F. J., Hannah, M. J., and Pyne, A. R., 1995, Geology of the margin of the Victoria Land basin off Cape Roberts, southwestern Ross Sea, *in* Cooper, A. K., Barker, P. F., and Brancolini, G., eds., Geology and seismic stratigraphy of the Antarctic margin: American Geophysical Union Antarctic Research Series, v. 68, p. 183–207.

Barron, J. A., Larsen, B., et al., eds., 1989, Proceedings of the Ocean Drilling Program, Scientific results: College Station, Texas (Ocean Drilling Program), v. 119, 1003 p.

Bartek, L. R., Henrys, S. A., Anderson, J. B., and Barrett, P. J., 1996, Seismic stratigraphy of McMurdo Sound, Antarctica: Implications for glacially influenced early Cenozoic eustatic change?: Marine Geology, v. 130, p. 79–98.

Berggren, W. A., and Prothero, D. R., 1992, Eocene–Oligocene climatic and biotic evolution: An overview, *in* Prothero, D. R., and Berggren, W. A., eds., Eocene–Oligocene climatic and biotic evolution: Princeton, New Jersey, Princeton University Press, p. 1–28.

Berggren, W. A., Kent, D. V., Flynn, J. J., and Van Couvering, J. A., 1985, Cenozoic geochronology: Geological Society of America Bulletin, v. 96, p. 1407–1418.

Berggren, W. A., Kent, D. V., Obradovich, J. D., and Swisher, C. C., III, 1992, Toward a revised Paleogene chronology, *in* Prothero, D. R., and Berggren, W. A., eds., Eocene–Oligocene climatic and biotic evolution: Princeton, New Jersey, Princeton University Press, p. 29–45.

Berggren, W. A., Kent, D. V., Swisher, C. C., III, and Aubrey, M.-P., 1995, A revised Cenozoic geochronology and biostratigraphy, *in* Berggren, W. A., Kent, D. V., Aubrey, M. P., and Hardenbol, J., eds., Geochronology, time scales, and stratigraphic correlation framework for an historical geology: SEPM (Society for Sedimentary Geology) Special Publication 54, p. 129–212.

Brinkhuis, H., 1992, Late Paleogene dinoflagellate cysts with special reference to the Eocene-Oligocene boundary, *in* Prothero, D. R., and Berggren, W. A., eds., Eocene–Oligocene climatic and biotic evolution: Princeton, New Jersey, Princeton University Press, p. 327–340.

Cande, S. C., and Kent, D. V., 1992, A new geomagnetic polarity time scale for the Late Cretaceous and Cenozoic: Journal of Geophysical Research, v. 97, p. 13917–13951.

Cande, S. C. and Kent, D. V., 1995, Revised calibration of the geomagnetic polarity time scale for the Late Cretaceous and Cenozoic: Journal of Geophysical Research, v. 100, p. 6093–6095.

Crouch, E. M., and Hollis, C. J., 1996, Paleogene palynomorph and radiolarian biostratigraphy of DSDP Leg 29, Sites 280 and 281, South Tasman Rise: Wellington, New Zealand, Institute of Geological and Nuclear Sciences Science Report, v. 96/19, 46 p.

Edwards, A. R., and Waghorn, D. B., 1989, Calcareous nannofossils, *in* Barrett, P. J., ed., Antarctic Cenozoic history from the CIROS-1 drillhole, McMurdo Sound, Antarctica: Wellington, New Zealand, DSIR Publishing, Department of Scientific and Industrial Research Bulletin, v. 245, p. 145–149.

Edwards, A. R., Hornibrook, N. B., Raine, J. I., Scott, G. H., Stevens, G. R., Strong, C. P., and Wilson, G. J., 1989, A New Zealand Cretaceous–Cenozoic time scale: Wellington, New Zealand, New Zealand Geological Survey Record, v. 35, p. 135–149.

Ehrmann, W. U., 1995, Clay mineral assemblages in Cenozoic sediments of Ross Sea, Antarctica: Sienna, Italy, International Symposium on Antarctic Earth Sciences, 7th, Abstracts and Proceedings, p. 118.

Ehrmann, W. U., 1997, Smectite concentrations and crystallinities: Indications for Eocene age of glaciomarine sediments in the CIROS-1 drill hole, McMurdo Sound, Antarctica, *in* Ricci, C.A., ed., Proceedings, VII International Symposium on Antarctic Earth Science: Sienna, Italy, p. 771–780.

Ehrmann, W. U., and Mackensen, A, 1992, Sedimentological evidence for the formation of an East Antarctic ice sheet in Eocene/Oligocene time: Palaeogeography, Palaeoclimatology, Palaeoecology, v. 93, p. 85–112.

Ehrmann, W. U., Melles, M., Kuhn, G., and Grobe, H., 1992, Significance of clay mineral assemblages in the Antarctic Ocean: Marine Geology, v. 107, p. 249–273.

Evitt, W. R., and Pierce, S. T., 1975, Early Tertiary ages from the coastal belt of the Franciscan Complex, northern California: Geology, v. 3, p. 433–436.

Fitzgerald, P. G., 1992, The Transantarctic Mountains of southern Victoria Land: The application of apatite fission track analysis to a rift shoulder uplift: Tectonics, v. 11, p. 634–662.

Goodman, D. K., and Ford, L. N., Jr., 1983, Preliminary dinoflagellate biostratigraphy for the middle Eocene to Lower Oligocene from the southwest Atlantic Ocean, *in* Ludwig, W. J., Krasheninikov, V. A., et al., eds., Initial reports of the Deep Sea Drilling Project: Washington, D.C., U.S. Government Printing Office v. 71, part 2, p. 859–877.

Hall, S. A., 1977, Cretaceous and Tertiary dinoflagellates from Seymour Island, Antarctica: Nature, v. 267, p. 239–241.

Hambrey, M. J., and Barrett, P. J., 1992, Cenozoic sedimentary and climatic record, Ross Sea region, Antarctica, *in* Kennett, J. P., and Warnke, D. A., eds., The Antarctic paleoenvironment: A perspective on global change, Part II: American Geophysical Union Antarctic Research Series, v. 60, p. 91–124.

Hambrey, M. J., Barrett, P. J., and Robinson, P. J., 1989, Stratigraphy, *in* Barrett, P. J., ed., Antarctic Cenozoic history from the CIROS-1 drillhole, McMurdo Sound, Antarctica: Wellington, New Zealand, DSIR Publishing, Department of Scientific and Industrial Research Bulletin, v. 245, p. 23–48.

Hannah, M. J., 1994, Eocene dinoflagellates from the CIROS-1 drill hole, McMurdo Sound Antarctica: Terra Antarctica, v. 1, p. 371.

Hannah, M. J., 1996, Eocene dinoflagellates from glacigenic strata cored in the CIROS-1 drillhole, McMurdo Sound, Antarctica: Dallas, Texas, American Association of Stratigraphic Palynologists, International Palynological Conference, 9th, Proceedings, p. 59.

Haq, B. U., Hardenbol, J., and Vail, P. R., 1988, Mesozoic and Cenozoic chronostratigraphy and cycles of sea-level change, *in* Wilgus, C. K, Hastings, B. S., Kendall, C. G. St. C., Posamentier, H., Ross, C. A., and van Wagoner, J., eds., Sea-level changes: An integrated approach: Society for Economic Paleontologists and Mineralogists Special Publication 42, p. 71–108.

Hartl, P., Tauxe, L., and Constable, C., 1993, Early Oligocene geomagnetic field behavior from Deep Sea Drilling Project Site 522: Journal of Geophysical Research, v. 98, p. 19649–19665.

Harwood, D. M., 1989, Siliceous microfossils, *in* Barrett, P. J., ed., Antarctic Cenozoic history from the CIROS-1 drillhole, McMurdo Sound, Antarctica: Wellington, New Zealand, DSIR Publishing, Department of Scientific and Industrial Research Bulletin, v. 245, p. 67–97.

Harwood, D. M., and Maruyama, T., 1992, Middle Eocene to Pleistocene diatom biostratigraphy of Southern Ocean sediments from the Kerguelen Plateau, Leg 120, *in* Wise, S. W., Jr., Schlich, R., et al., eds., Proceedings of the Ocean Drilling Program, Scientific results: College Station, Texas (Ocean Drilling Program), v. 120, p. 683–733.

Harwood, D. M., Barrett, P. J., Edwards, A. R., Rieck, H. J., and Webb, P.-N., 1989, Biostratigraphy and chronology, *in* Barrett, P. J., ed., Antarctic Cenozoic history from the CIROS-1 drillhole, McMurdo Sound, Antarctica: Wellington, New Zealand, DSIR Publishing, Department of Scientific and Industrial Research Bulletin, v. 245, p. 231–239.

Hayes, D. E., Frakes, L. A., et al., eds., 1975, Initial reports of the Deep Sea Drilling Project: Washington, D.C., U.S. Government Printing Office, v. 28, 1017 p.

Henrys, S. A., Bartek, L. R., Anderson, J. B., and Barrett, P. J., 1991, Seismic stratigraphy in McMurdo Sound: Correlation of high resolution data sets: Terra Antarctica, v. 1, p. 373–374.

Hill, R. S., 1989, Fossil leaf, *in* Barrett, P. J., ed., Antarctic Cenozoic history from the CIROS-1 drillhole, McMurdo Sound, Antarctica: Wellington, New Zealand, DSIR Publishing, Department of Scientific and Industrial Research Bulletin, v. 245, p. 143–144.

Jenkins, D. G., 1985, Southern mid-latitude Paleocene to Holocene planktic foraminifera, *in* Bolli, H. M., Saunders, J. B., and Perch-Nilsen, K., eds., Plankton stratigraphy: Cambridge, United Kingdom, Cambridge University Press, p. 263–281.

Kemp, E. M., 1975, Palynology of Leg 28 drill sites, *in* Hayes, D. E., Frakes, L. A., et al., eds., Initial reports of the Deep Sea Drilling Project: Washington, D.C., U.S. Government Printing Office, v. 28, p. 599–621.

Kennett, J. P., 1977, Cenozoic evolution of Antarctic glaciation, the circum-Antarctic ocean, and their impact on global paleoceanography: Journal of Geophysical Research, v. 82, p. 3843–3860.

Lanci, L., Lowrie, W., and Montanari, A., 1996, Magnetostratigraphy of the Eocene/Oligocene boundary in a short drill-core: Earth and Planetary Science Letters, v. 143, p. 37–48.

Lawver, L. A., Gahagan, L. M., and Coffin, M. F., 1992, The development of paleoseaways around Antarctica, *in* Kennett, J. P., and Warnke, D. A., eds., The Antarctic paleoenvironment: A perspective on global change, Part I: American Geophysical Union Antarctic Research Series, v. 58, p. 7–30.

Lowrie, W, 1990, Identification of ferromagnetic minerals in a rock by coercivity and unblocking temperature properties: Geophysical Research Letters, v. 17, p. 159–162.

McIntyre, D. J., and Wilson, G. J., 1966, Preliminary palynology of some Antarctic Tertiary erratics: New Zealand Journal of Botany, v. 4, p. 315–321.

Miller, K. G., 1992, Middle Eocene to Oligocene stable isotopes, climate, and deep water history: The terminal Eocene event, *in* Prothero, D. R., and Berggren, W. A., eds., Eocene–Oligocene climatic and biotic evolution: Princeton, New Jersey, Princeton University Press, p. 131–159.

Miller, K. G., Feigenson, M. D., Kent, D. V., and Olsson, R. K., 1988, Upper Eocene to Oligocene isotope ($^{87}Sr/^{86}Sr$, $\delta^{18}O$, $\delta^{13}C$) Standard section, Deep Sea Drilling Project Site 522: Paleoceanography, v. 3, p. 223–233.

Mohr, B. A. R., 1990, Eocene and Oligocene sporomorphs and dinoflagellate cysts from Leg 113 drill sites, Weddell Sea, Antarctica, *in* Barker, P. F., Kennett, J. P., et al., eds., Proceedings of the Ocean Drilling Program, Scientific results: College Station, Texas (Ocean Drilling Program), v. 113, p. 595–612.

Nocchi, M., Parisi, G., Monaco, P., Monechi, S., Mandile, M., Napoleone, G., Ripepe, M., Orlando, M., Premoli-Silva, I., and Bice, D. M., 1986, The Eocene-Oligocene boundary in the Umbrian pelagic recession, *in* Pomerol, C., and Premoli-Silva, I., eds., Terminal Eocene events: Amsterdam, Netherlands, Elsevier, p. 25–40.

Prothero, D. R., and Berggren, W. A., eds., 1992, Eocene–Oligocene climatic and biotic evolution: Princeton, New Jersey, Princeton University Press, 568 p.

Rieck, H. J., 1989, Paleomagnetic stratigraphy, *in* Barrett, P. J., ed., Antarctic Cenozoic history from the CIROS-1 drillhole, McMurdo Sound, Antarctica: Wellington, New Zealand, DSIR Publishing, Department of Scientific and Industrial Research Bulletin, v. 245, p. 153–158.

Sagnotti, L., Florindo, F., Verosub, K. L., Wilson, G. S., and Roberts, A. P., 1996, Environmental magnetic record of Antarctic paleoclimate from Eocene–Miocene glaciomarine sediments, Victoria Land margin: Eos (Transactions, American Geophysical Union), v. 77, supplement, p. 163.

Shackleton, N. J., and Kennett, J. P., 1975, Paleotemperature history of the Cenozoic and the initiation of Antarctic glaciation: Oxygen and carbon isotope analyses in DSDP Sites 277, 279 and 281, *in* Kennett, J. P., Houtz, R. E. et al., eds., Initial reports of the Deep Sea Drilling Project: Washington, D.C., U.S. Government Printing Office, v. 29, p. 743–756.

Stover, L. E., and Williams, G. L., 1995, A revision of the Paleogene dinoflagellate genera *Areosphaeridium* Eaton (1971) and *Eatonicysta* Stover and Evitt (1978): Micropaleontology, v. 41, p. 97–141.

Turner, G. M. and Bryant, I. D., 1995, Application of paleomagnetic reversal stratigraphy to constrain well correlation and sequence stratigraphic interpretation of the Eocene C1 Sands, Maui Field, New Zealand, *in* Turner, P., and Turner, A., eds., Palaeomagnetic applications in hydrocarbon exploration and production: Geological Society [London] Special Publication 98, p. 205–221.

Webb, P.-N., 1989, Benthic foraminifera, *in* Barrett, P. J., ed., Antarctic Cenozoic history from the CIROS-1 drillhole, McMurdo Sound, Antarctica: Wellington, New Zealand, DSIR Publishing, Department of Scientific and Industrial Research Bulletin, v. 245, p. 99–118.

Webb, P.-N., and Wilson, G. S., eds., 1994, The Cape Roberts Project, Antarctic stratigraphic drilling, proceedings of the U.S. planning workshop science objectives and requirements meeting: Byrd Polar Research Center Report Series, v. 10, 117 p.

Wei, W., 1991, Evidence for an earliest Oligocene abrupt cooling in the surface waters of the Southern Ocean: Geology, v. 19, p. 780–783.

Wei, W., 1992, Updated nannofossil stratigraphy of the CIROS-1 core from McMurdo Sound (Ross Sea), *in* Wise, S. W., Jr., Schlich, R., et al., eds., Proceedings of the Ocean Drilling Program, Scientific results, College Station, Texas (Ocean Drilling Program), v. 120, p. 1105–1117.

Wei, W., and Thierstein, H. R., 1991, Upper Cretaceous and Cenozoic calcareous nannofossils of the Kerguelen Plateau (southern Indian Ocean) Prydz Bay (East Antarctica), *in* Barron, J., Larsen, B., et al., eds., Proceedings of the Ocean Drilling Program, Scientific results: College Station, Texas (Ocean Drilling Program), v. 119, p. 467–487.

Wei, W., and Wise, Jr., S. W., 1990, Middle Eocene to Pleistocene calcareous nannofossils recovered by Ocean Drilling Program Leg 113 in the Weddell Sea, *in* Barker, P. F., Kennett, J. P., et al., eds., Proceedings of the Ocean Drilling Program, Scientific results: College Station, Texas (Ocean Drilling Program), v. 113, p. 639–666.

Williams, G. L., and Bujak, J. P., 1985, Mesozoic and Cenozoic dinoflagellates, *in* Bolli, H. M., Saunders, J. B., and Perch-Nielsen, K., eds., Plankton stratigraphy: Cambridge, United Kingdom, Cambridge University Press, p. 847–964.

Wilson, G. J., 1967, Some new species of lower Tertiary dinoflagellates from McMurdo Sound, Antarctica: New Zealand Journal of Botany, v. 5, p. 57–83.

Wilson, G. J., 1989, Marine palynology, *in* Barrett, P. J., ed., Antarctic Cenozoic history from the CIROS-1 drillhole, McMurdo Sound, Antarctica: Wellington, New Zealand, DSIR Publishing, Department of Scientific and Industrial Research Bulletin, v. 245, p. 129–133.

Wilson, G. J., and Clowes, C. D., 1982, *Arachnodinium*, a new dinoflagellate genus from the lower Tertiary of Antarctica: Palynology, v. 6, p. 97–103.

Wise, S. W., Jr., Breza, J. R., Harwood, D. M., and Wei, W., 1991, Paleogene glacial history of Antarctica, *in* Muller, D. W., McKenzie, J. A., and Weissert, H., eds., Controversies in modern geology: New York, Academic Press, p. 133–171.

Wood, K. C., Miller, K. G., and Lohmann, G. P., 1985, Middle Eocene to Oligocene benthic foraminifera from the Oceanic Formation, Barbados: Micropaleontology, v. 31, p. 181–196.

Wrenn, J. H. and Hart, G. F., 1988, Paleogene dinoflagellate cyst biostratigraphy of Seymour Island, Antarctica, *in* Feldmann R. M., and Woodburne, M. O., eds., Geology and paleontology of Seymour Island, Antarctic Peninsula: Geological Society of America Memoir 169, p. 321–447.

MANUSCRIPT RECEIVED BY THE SOCIETY JANUARY 29, 1997
REVISED MANUSCRIPT RECEIVED APRIL 30, 1997
MANUSCRIPT ACCEPTED MAY 15, 1997

Printed in U.S.A.